한국기계가공학회지, 제17권, 제5호, pp.37～44(2018.10) ISSN 1598-6721(Print)
Journal of the Korean Society of Manufacturing Process Engineers, Vol. 17, No. 5, pp.37~44(2018.10) ISSN 2288-0771(Online)

https://doi.org/10.14775/ksmpe.2018.17.5.037

Analysis of Heat Transfer by Various Laser Beam Patterns in Laser Material Process

Hae-Woon Choi*,#

*Dept. of Mechanical and Automotive Engineering, Keimyung University

가변 레이저 빔 패턴에 따른 열영향 해석

최해운*,#

*계명대학교 기계자동차공학과

(Received 28 April 2018; received in revised form 8 July 2018; accepted 12 July 2018)

ABSTRACT

In laser material processing for high thermal conductivity, the thermal effect of laser beam shape was examined through computer simulations. In this paper, a circular beam with a focal radius of 500 μm, an elliptical beam with a major axis of 4 mm and a minor axis of 1 mm, and a rotating beam with a focal radius of 500 μm and an angular velocity of 5 rad/sec were compared. Simulation results showed that there was no clear difference in the maximum temperature between the circular focus and the elliptical shape, but the heating and cooling rates were different. The simulation result for a laser beam rotating in a circular pattern with a radius of 5 mm showed an asymmetric temperature rise due to the combination of linear and rotational motion. At points where the rotational and linear speeds combined, the temperature gradually rose and reached the maximum temperature; whereas at points where the rotational and linear speeds were attenuated, the temperature tended to gradually decrease after reaching the maximum temperature. Based on the results of this study, the authors expect to be able to optimize laser material processing by designing patterns of laser beams.

Key words: Computer Simulation(시뮬레이션), Laser Material Process(레이저 가공), Laser Beam Shape(레이저 빔 형상제어, Optimum Design(최적설계)

1. Introduction

Aluminum, a representing material as lightweight metal, has been widely used in fields where high strength and light weight are required such as the automotive and aviation industries. Its is only one-third of that of steel by weight, but its fatigue characteristics and thermal conductivity are superior, so its utilization rate is very high[1–3].

To reduce fuel consumption, maintenance costs, and operating costs, necessary of lightweight design has increased in various industries. Thus, the application of aluminum as a lightweight material is expected to rise further in the future. In particular, the improvement of fuel economy in the automotive

Corresponding Author : hwchoi@gw.kmu.ac.kr
Tel: +82-53-580-5216, Fax: +82-53-580-6067

industry is necessary due to the requirement of a reduction in maintenance costs as well as environmental issues, the utilization of aluminum is futher required [2–3].

Automotive parts should ensure high reliability, low cost, and high productivity simultaneously. In particular, since the attachment or welding of various types of materials is used to reduce the manufacturing cost to meet consumer demand, materials that can minimize machine processing are desired. However, there have been limitations on applying various welding methods to processes for high thermal conductivity and a low melting point, such as aluminum due to their internal structural characteristics[3–4]. To solve these issues, process control of the heat input during the welding of steel and aluminum needs to be studied. Recently a technique that employs a laser that has high energy density and facilitates precise control has been widely used for dissimilar material bonding[2–4].

Despite the high thermal conductivity and surface reflectivity of aluminum, a laser beam is advantageous due to high-density energy input in a local area in a short period of time. However, there are still problems to overcome such as defects that occur in the process, which are undercuts due to internal porosity or surface bubbles. To overcome this limitation, studies have been conducted by other researchers using a laser beam to vary the shape[5–6].

Studies have also been conducted to raise the processing efficiency by adjusting beam shape and size as well as transfer to controlling the high energy density, in which a focal point was moved to the right or left or rotated circularly to distribute the energy, thereby obtaining results that could not be acquired in previous processes.

The effect of the laser beam vibration pattern (horizontal, vertical, and circular) on the aluminum (AA6061-T6) has been reported and verified that the highest-reliability welding results could be acquired with circular pattern vibration[6].

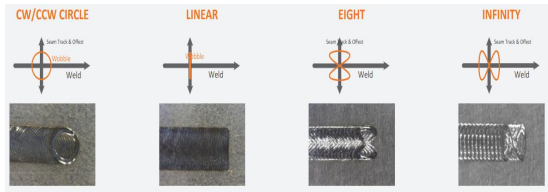

Fig. 1 Examples of beam scanning pattern[7]

In addition, the experimental studyshowed that no significant difference in tensile strength was found due to the laser beam vibration, but the toughness was increased[6].

In addition to studies on the beam pattern, other variable study results have also been reported after applying a laser heat source by separating or overlapping the heat source. In galvanized steel sheet and aluminum alloy thin-film welding, a robust and uniform brazing bead with high surface quality could be obtained at a high welding speed when laser welding and the brazing process were used in the double-beam mode[5]. The developed techniques have been commercialized and utilized in various fields (Fig. 1).

This paper reports a model that can minimize trial and error in the process design by predicting the results according to various laser beam patterns in a virtual space through computer simulations.

2. Theoretical background and modeling

The commercial FEM program was used to analyze the thermal effect due to beam shapes via a numerical analysis method (COMSOL ver. 5.2). The heat input used in the simulation was a three-dimensional (3D) heat input energy model, which was modeled considering the “skin depth” of the heat input energy in addition to a two-dimensional (2D) elliptical heat source, which was reduced to 1/e (approximately 0.37) or lower. Generally, the skin depth is calculated via Eq. (1) according to the applied electromagnetic wavelength

and electric characteristics. The skin depth of aluminum or copper with regard to a laser in the visible light range was only several nanometers. Thus, it was assumed to be 50㎛ in this simulation for the simplicity.

$$\delta = \sqrt{\frac{\psi}{\pi f \mu}} \quad (1)$$

Here, ψ refers to electric resistivity and μ refers to the relative permeability. In addition, the 2D heat source shape is represented as presented in Eq. (2)[8–9].

$$Q(x,y,z) = Q_0(1-R_c)\frac{A_c}{\pi\sigma_x\sigma_y} e^{-\left[\frac{(x-x_0)^2}{2\sigma_x^2}+\frac{(y-y_0)^2}{2\sigma_y^2}\right]} . e^{-A_c z} \quad (2)$$

Here, Q_0 refers to the peak output of the heat source, (x,y,z) refers to the space coordinates, R_c refers to the surface reflectivity, σ_x and σ_y refer to the beam radii in the x and y directions, and A_c refers to the thickness of the surface absorption layer. For the boundary conditions, a laser was irradiated from above, and a natural convection condition was set in the whole surface. The heat transfer-governing equation for inside aluminum is expressed by Eq.(3)[9–10].

$$\rho C_p \frac{\partial T}{\partial t} + \rho C_p u \cdot \nabla T = \nabla \cdot (k \nabla T) + Q \quad (3)$$

Here, ρ is the density, C_p is the specific heat, T is the temperature, u is the velocity vector, and Q is the heat flux. The heat source was assumed to be a standard normal distribution (Gaussian). The beam-shape factor was set to two, and the laser output was set to 1 kW.

Three types of simulations were conducted. The detailed simulation method is depicted in Fig. 2. The material used in the simulation was assumed to be 1-mm-thick, 50-mm-wide, and 100-mm-long aluminum (AL-6063). Its detailed physical properties are summarized in Table 1.

Table 1 Material properties of AL6063[11]

Property	Value	Unit
Heat capacity(Cp)	900	J/(kg.K)
Density(ρ)	2700	kg/m^3
Thermal conductivity($\varkappa$)	201	W/m.K
Rel. permeability(μ)	1	
Elec. conductivity(ξ)	2.03x10^7	S/m
Thermal exp. Coeff.(α)	23.4x10^{-6}	1/K

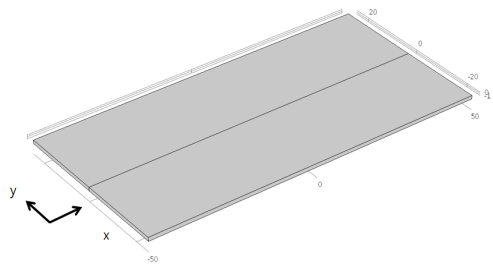

(a) Simulation model

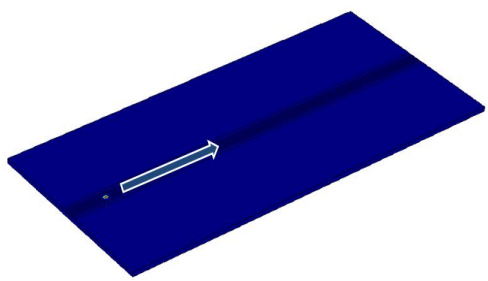

(b) focused beam with linear motion

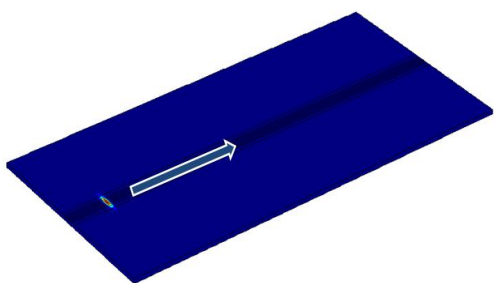

(c) elliptical beam with linear motion

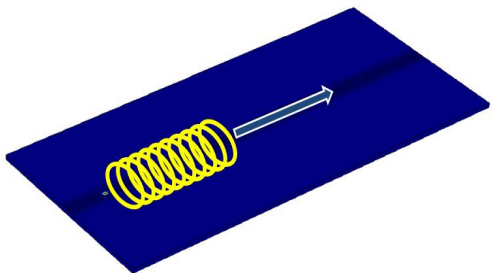

(d) focused beam with circular motion

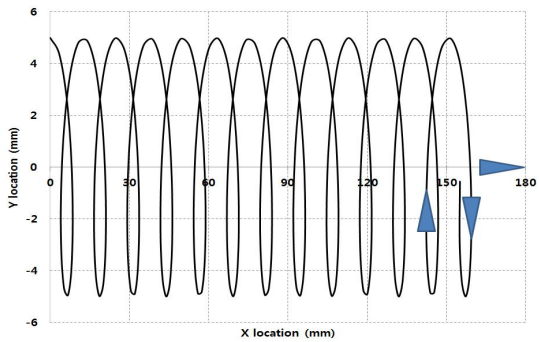

(e) trajectory of laser beam

Fig. 2 Simulation model and beam patterns

Table 2 Beam profiles and motion description

Variables	Case 1	Case 2	Case 3
Beam shape	Cir	Ellip	Cir
Motion	Linear	Linear	Cir
Scan speed(mm/s)	10	10	10
Rot speed(rad/sec)	None	None	5
Rad. of circle(mm)	None	None	5mm

The heat source was set to the following three cases. As shown in Fig. 2(b), a circular beam with a focal radius of 500 ㎛ was directly transferred at 10 mm/sec (Case 1). As shown in Fig. 2(c), an elliptical beam with a major axis (y-direction) of 4 mm and a minor axis (x-direction) of 1 mm was directly transferred at 10 mm/sec (Case 2).

As shown in Fig.2(d), a circular beam with a focal radius of 500㎛ was directly transferred at the speed of 10 mm/sec while rotating with an angular velocity of 5 rad/sec in the clockwise direction with a radius of 5 mm (Case 3). In Case 3, a laser beam was transferred linearly at 10 mm/sec while rotating so that it was transferred in a spiral form, as shown in Fig. 2(e). Table 2 summarizes the conditions of the beam shape and transfer speed for each case in detail.

In addition, the probing point was set to +/-2 mm in the y direction at the center to compare the real-time temperature changes according to the laser beam shape quantitatively.

3. Simulation results

Three types of simulations were conducted as presented in Table 2. Generally, in the case laser welding, a convection transfer of a large amount of energy transer occurs in a melting pool due to the heat transfer caused by the conduction inside the metal as well as the molten metal flow. However, the present study limited to only a simple comparison of the thermal transfer effect due to the focusing beam, elliptical beam, and rotation of the focusing beam.

This study conducted simulations as shown in Fig. 2(b). In the simulation, a laser beam was assumed to be a line beam, and the type of laser beam was a long elliptical shape that had a long and short axes ratio of 4:1.

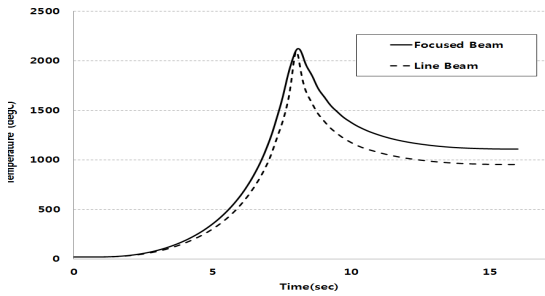

Fig. 3 Temperature distribution by linear moving beam (focused vs. elliptical beam)

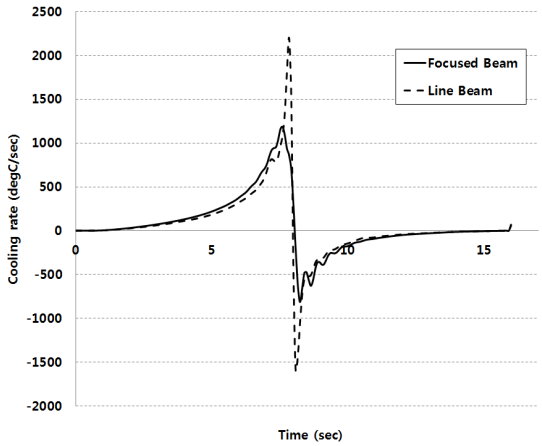

Fig. 4 Heating and Cooling rate

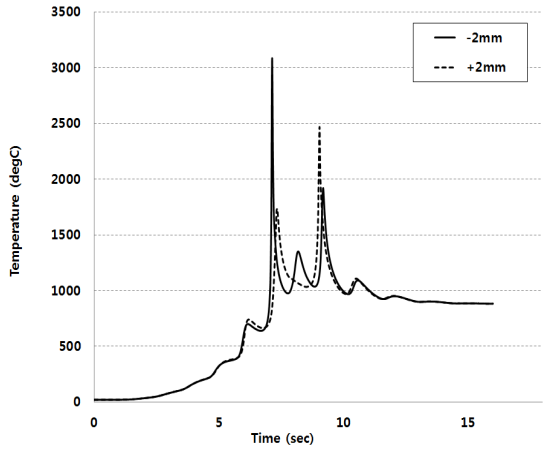

Fig. 5 Temp. distribution (oscillating beam)

To determine the effects of beams focused with the focusing and elliptical shapes, the temperatures in the ± 2-mm offset region in the y direction from the center axis were compared, and the results are shown in Fig. 3.

As compared in Fig. 3, the highest temperature of the laser focused with the elliptical shape was not significantly different from that of the laser focused with a circular focus. Here, the temperature gradient in the corresponding section was analyzed to determine the difference in the heating and cooling rates, as shown in Fig. 4. The results showed that the laser focused with an elliptical shape had a steeper rise and drop than those of the laser focused with a circular focus. As shown in Fig. 4, the heating and cooling rates at the peak were twice as high in the elliptical beam than in the circular beam.

This result was due to the difference in energy density, which is reasonable, although there were many other affeting variables. That is, the total output of the irradiated laser was the same, but the area of the elliptical shape was four times larger than the circular focusing area so that the total energy density irradiated was distributed uniformly by 1/4 proportionally.

This result verified that when a laser beam's shape changed, not only can the energy density be controlled, but the heating and cooling rates applied to the material can also be controlled. This effect is expected to vary to some extent according to whether the area of interest (y= ±2mm) is included in the laser beam region (±2mm). That is, when the bead width is 4 mm, a similar effect will be obtained with the minimum line beam width of 4 mm.

Fig. 5 shows the simulation of Fig. 2(e), in which the temperature distribution at the measurement point was measured when the circular beam of the focal radius 500 ㎛ was directly transferred at 10 mm/sec while rotating in a 5-mm radius in the clockwise direction at 5 rad/sec.

It should be noted in the simulation results that measurement point y was symmetrical around the center, but the temperature distribution was not symmetrical. This was in contrast with the symmetry of the temperature distribution in the circular focusing laser or elliptical laser beam. The maximum temperature at the y= +2mm point was 2,500℃, whereas the maximum temperature at y= -2mm was 3,050℃. These results indicated that a significant temperature difference occurred depending

on the symmetrical measurement point location even if the error due to the minimum size limitation in the FEM was considered. The imbalance of the temperature distribution was due to the speed imbalance that occurred t the measurement point. The displacement and velocity vectors were calculated to analyze this numerically. The displacement vector is expressed by Eq. (3), and momentary displacement, that is, the velocity vector, is expressed by Eq. (4).

As inferred by the equations, the rotational linear velocity of the laser beam and linear velocity were combined in the case of y = +2mm, which accelerated the velocity. In contrast, the rotational linear velocity had a delay effect on the laser beam in the travel direction in the case of y = -2mm.

$$\vec{r}_{x,y} = r_0[\sin(wt)\vec{i} + \cos(wt)\vec{j}] + v_0 t\vec{i} \qquad (3)$$

$$\vec{v}_{x,y} = -r_0 w[\cos(wt)\vec{i} - \sin(wt)\vec{j}] + v_0\vec{i} \qquad (4)$$

The change in velocity from Eq. (4) can be calculated as shown in Fig. 6. In the case of positions y = +2mm and y = -2mm, the calculated changes were υ= +35 mm/sec and υ= -15 mm/sec. That is, at the location of y = +2 mm, the rotational linear velocity (or tangential velocity) and the straight velocity were combined to cause acceleration. In contrast, at the location of y = -2 mm, the directions of the straight velocity and rotational velocity were the opposite so that the laser beam was transferred in the opposite direction, thereby having the effect of supplying an additional heat source.

It should also be noted that the temperature rose gradually and reached the maximum temperature at the location of y = +2 mm. In contrast, at the location of y = -2 mm, the temperature tended to gradually drop after reaching the maximum temperature. These results can also be inferred from Eq. (4).

Based on the analysis of results, if the laser beam was rotated in the counter-clockwise direction rather than in the clockwise direction, the results would be produced in the opposite manner. Conclusively, the “gradual rise or drop” of the heat impact applied to the material due to the beam shape and rotation can be estimated in advance through simulations.

Finally, an isotherm contour was tracked to determine the heat flow (heat flux) during or after heating. By tracking the vector that was orthogonal to the isotherm contour, a stream line of the heat expansion direction could be calculated, through which information about the heating and cooling gradients could be obtained.

As shown in Fig. 7(a), the circularly rotated laser beam did not have symmetry in the travel direction, and the heat flux was steeply formed in the travel direction. In particular, as shown in Fig. 7(b), the heat flux around the focal point changed rapidly according to the laser beam travel direction, and an optimal processing design can be achieved by considering the heat flux by utilizing the above results.

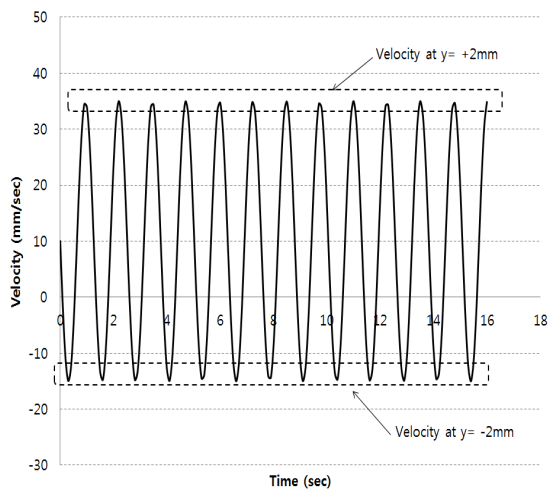

Fig. 6 Velocity respect to the x-direction

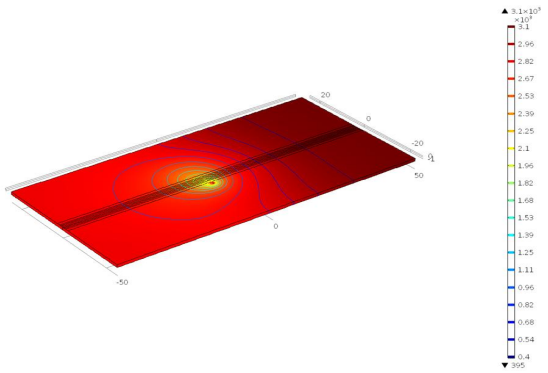

(a) Contours of isotherm (Max. Temp. 3,100K)

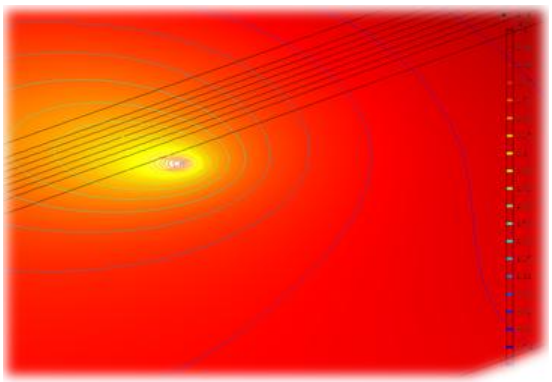

(b) laser beam irradiation

Fig. 7 Contours of isotherms

4. Conclusions

This study reported the heat effect results according to a laser heat source shape in the laser processing of materials whose heat conductivity was relatively high. In heat flows during real welding, not only heat flow due to conduction occurred, but also heat transfer due to phase change and fluid convection, which occurred frequently. However, this study analyzed the effect of the beam shape only, which is a limitation.

The circular laser beam with a focal radius of 500 ㎛, the elliptical beam with a 4-mm long axis and 1-mm short axis, and the rotating beam at an angular velocity of 5 rad/sec with a focal radius of 500 ㎛ were compared and analyzed. There was no temperature difference between the laser beams focused with a circular focus and elliptical shape, but there was a difference in their heating and cooling rates.

In contrast, the laser focused with a circular focus was rotated at an angular velocity of 5 rad/sec with a radius of 5 mm, and then a temperature rise occurred in the symmetrical form due to the combination of the linear and rotational transfer speed.

In particular, the rotation result in a circular shape exhibited that the temperature rose gradually in the region (y = +2 mm) where the rotational and linear speed were combined, thereby reaching the maximum temperature. In contrast, in the decreasing speed region (y = -2 mm) where the rotational and linear speed traveled in the opposite direction, the temperature tended to drop gradually after rising to the maximum temperature. This effect indicated that the laser beam effect will differ according to the normal and reverse rotations and can be applied effectively to a thermal effect analysis of dissimilar metals whose heat conductivity differs.

Acknowledgment

"This study was supported by the 2017 Bisa Research Grant (Sabbatical year) in Keimyung University."

REFERENCES

1. Dursun, T., "Recent Developments in Advanced Aircraft Aluminium Alloys," Materials and Design, 56, pp. 862-871, 2014.
2 Kessler, F., "Fiber Laser Welding in the Car Body Shop," Journal of Welding and Joining, Vol. 31, No. 4, pp. 17-22, 2013.

3. Wang, P., Chen, X., Pan, Q., Madigan, B. and Long, J., “Laser welding dissimilar materials of aluminum to steel: an overview,” Int. Journal of Adv. Manufacturing Technology, 87, pp. 3081-3091, 2016.
4. Brown, R., Tang, W., and Reynolds, A. “Multi-pass friction stir welding in alloy 7050-T7451: Effects on weld response variables and on weld properties,” Materials Science and Engineering A 513–514, pp. 115–121, 2009.
5. Mohammadpour, M., Yazdian, N., Yang, G., Wang, H., Carlson, B. and Kovacevic, R., “Effect of dual laser beam on dissimilar welding-brazing of aluminum to galvanized steel,” Optics and Laser Technology, 98, pp. 214-228, 2018.
6. Wang, L., Gao, M., Zhanga, C. and Zeng, X., “Effect of beam oscillating pattern on weld characterization of laser welding of AA6061-T6 aluminum alloy,” Materials and Design, 108, pp. 707-717, 2016.
7. Technical Brochure, IPG Photonics 2018, www.ipgphotonics.com, 2018.
8. Choi, H. and Yoon, S., “Laser Welding Analysis for 3D Printed Thermoplastic and Poly-acetate Polymers,” Trans. Korean Soc. Mech. Eng. A, Vol. 39, No. 7, pp. 701-706, 2015.
9. Lee, S. T., Park, S. G., and Choi, H W., “CFRP Laser Joining Computer Simulation in a Parallel Kinematic Machine,” Journal of the Korean Society of Manufacturing Process Engineers, Vol. 16, No. 1, pp.77-82, 2017.
10. Lee, D., Park, K. and Kang, D., “A Study on the Finite Element Analysis in Friction Stir Welding of Al Alloy,” Journal of the Korean Society of Manufacturing Process Engineers, Vol, 14, No. 5, pp.81-87, 2015.
11. COMSOL Multiphysics reference manual, Heat Transfer. www.comsol.com, 2018.